JOURNAL OF MODERN OPTICS, 1988, VOL. 35, NO. 11, 1741–1755

Accurate numerical solution of the fourth-moment equation for very large values of Γ

M. SPIVACK and B. J. USCINSKI

Department of Applied Mathematics and Theoretical Physics,
University of Cambridge, Silver Street, Cambridge CB3 9EW, England

(*Received 5 February 1988 and accepted 24 March 1988*)

Abstract. The parabolic fourth-moment equation is integrated numerically using a method based on operator splitting. The numerical scheme is unconditionally stable and convergent, allowing accurate results to be obtained for very large values of the strength parameter Γ. Intensity fluctuation spectra are obtained for values of Γ up to 10^5, three orders of magnitude larger than previously achieved. These spectra are compared with analytical solutions. Laws governing the position and height of the scintillation index peak are deduced.

1. Introduction

In recent years there has been considerable progress in the study of intensity fluctuations that arise when a wave propagates through a randomly irregular medium. Analytical solutions have been found for the fourth-moment equation, giving the space-time spectrum of such fluctuations [1–5]. The fourth-moment equation has also been integrated numerically using various methods [6–9]. The numerical solutions have, however, been confined to relatively small values of the strength parameter Γ, that is to media in which the scattering per unit scaled propagation distance Z is not very large. Moreover, no systematic comparison has been made between the numerical and analytical solutions. The present paper presents accurate numerical solutions for a very large range of values of Γ and compares these results with the analytical solutions for the intensity fluctuation spectrum.

The numerical scheme introduced in the present paper is based on a method of operator splitting and gives reliable results for values of Γ up to 10^5. This is three orders of magnitude larger than those appearing in previously published numerical solutions. The method is quasi-analytical in its nature and is unconditionally stable and convergent. It has the merit of allowing the numerical and analytical intensity fluctuation spectra to be compared over a wide range of Γ and Z, thus helping to establish the regions of validity and usefulness of both approaches.

Finally the wide range of validity of the numerical solutions allows us to establish certain simple functional relationships that govern the behaviour of the position and height of the peak appearing in the curve of the scintillation index.

2. The fourth-moment equation

A medium whose refractive index is

$$n(x, z) = \langle n \rangle + \mu n_1(x, z) \tag{1}$$

occupies the half-space ($z>0$) of a Cartesian set of coordinates (x, z). Angle brackets denote an ensemble average, and n_1 is a homogeneous and isotropic Gaussian random variable with zero mean and unit variance. A plane wave of wavenumber $k=2\pi/\lambda$ travelling in the positive z direction is normally incident on the medium. It has been shown by several authors [9, 10, 4] that m, the fourth moment of the wave-field $E(x, z)$, given by

$$m=\langle E(x_1, z)E^*(x_2, z)E(x_3, z)E^*(x_4, z)\rangle, \tag{2}$$

obeys the equation

$$\frac{\partial m}{\partial Z}=-\mathrm{i}\frac{\partial^2 m}{\partial\xi\partial\eta}-2\Gamma[1-g(\xi;\eta)]m, \tag{3}$$

where

$$\left.\begin{aligned}\xi&=(x_1-x_2-x_3+x_4)/2L,\\ \eta&=(x_1+x_2-x_3-x_4)/2L,\\ Z&=z/kL^2,\end{aligned}\right\} \tag{4}$$

and L is the scale size of the refractive-index irregularities

$$g(\xi;\eta)=f(\xi)+f(\eta)-\tfrac{1}{2}f(\xi+\eta)-\tfrac{1}{2}f(\xi-\eta). \tag{5}$$

Here f is the normalized spatial autocorrelation function of the refractive-index irregularities

$$f(\xi)=\rho(\xi)/\rho(0),$$

$$\rho(\xi)=\int_{-\infty}^{\infty}\langle n_1(x+\xi, z')n_1(x, z'')\rangle\,\mathrm{d}(z'-z''), \tag{6}$$

and Γ the strength parameter is defined by

$$\Gamma=k^3\mu^2\rho(0)L^2. \tag{7}$$

We shall find the numerical solution $m(\xi, \eta, Z)$ of (3) for the initial condition

$$m(\xi, \eta, 0)=1,$$

using the fact that it has the following symmetry properties

$$m(\xi, \eta, Z)=m^*(\xi, -\eta, Z)=m^*(-\xi, \eta, Z). \tag{8}$$

If $I_i=EE^*$ is the intensity at the point (x_i, z) then the spatial autocorrelation function of intensity fluctuations is

$$\rho_I^2=\langle I_1I_2\rangle-1=m(\xi, 0, Z)-1, \tag{9}$$

and the scintillation index is

$$\sigma_I^2=\langle I^2\rangle-1=m(0, 0, Z)-1. \tag{10}$$

In the course of obtaining numerical and analytical solutions it is convenient to represent the fourth moment $m(\xi, \eta, Z)$ in terms of its Fourier transform $M(\nu_1, \nu_2, Z)$

$$m(\xi, \eta, Z)=\int_{-\infty}^{\infty}\int_{-\infty}^{\infty}M(\nu_1, \nu_2, Z)\exp[\mathrm{i}(\nu_1\xi+\nu_2\eta)]\,\mathrm{d}\nu_1\,\mathrm{d}\nu_2. \tag{11}$$

Thus the intensity correlation in (9) can be written as

$$m(\xi, 0, Z) = \int M(\nu_1, Z) \exp(\mathrm{i}\nu_1 \xi)\, \mathrm{d}\nu_1, \tag{12}$$

where

$$M(\nu_1, Z) = \int M(\nu_1, \nu_2, Z)\, \mathrm{d}\nu_2. \tag{13}$$

Thus $M(\nu_1, Z)$ is the spatial frequency spectrum of the intensity fluctuations. In what follows, the subscript will be omitted from ν_1 to simplify the notation since ν_2 now no longer appears.

3. Numerical solution

We can write equation (3) in terms of operators as

$$\partial m/\partial Z = [A(Z) + B(\Gamma, Z)]m, \tag{14}$$

where

$$A = -\mathrm{i}\frac{\partial^2}{\partial\xi\partial\eta}, \quad B = -2\Gamma[1 - g(\xi, \eta)].$$

We can write $C = A + B$. Difficulties can arise in the numerical solution for C, particularly for large values of Γ, when semi-discretization leads to a stiff system of differential equations. Furthermore, since there are two transverse dimensions, the matrices which operate on this system are of order N^4, where N is the number of points in the discretization along each axis.

The formal solution of (14) over the range $(Z, Z + \Delta Z)$ is

$$m(\xi, \eta, Z + \Delta Z) = \exp\left[\int_Z^{Z+\Delta Z} C(\Gamma, Z')\, \mathrm{d}Z'\right] m(\xi, \eta, Z).$$

In the case of a plane wave, C does not vary with Z and so $\int C\, \mathrm{d}Z = \Delta Z C$. We first approximate $\exp[\Delta Z C]$ by

$$\exp(\Delta Z C) \approx \exp(\Delta Z A) \exp(\Delta Z B). \tag{15}$$

This is analogous to the split-step solution used in the simulation of random wave propagation [11, 12]. It is exact only if A and B commute. An explicit analytical expression can now easily be obtained for $\exp(\Delta Z A)$, and $\exp(\Delta Z B)$ is just the multiplication operator $\exp[-2\Gamma\Delta Z(1 - g)]$. The solution for $\exp(\Delta Z A)$ can be found by taking the Fourier transform of the equation $\partial m/\partial Z = Am$. If we denote the Fourier transform operator by $\mathscr{F}$ and the transform variables by ν_1 and ν_2 then

$$exp(\Delta Z A) m(\xi, \eta) = \mathscr{F}^{-1}[\exp[\mathrm{i}\nu_1\nu_2 \Delta Z]\mathscr{F}(m)]. \tag{16}$$

This can be handled numerically by use of the fast Fourier transform (FFT) provided that we can deal effectively with boundaries. The boundary conditions are treated analytically, as explained below.

To implement this scheme, the solutions for $\exp(\Delta Z B)$, $\exp(\Delta Z A)$ are applied alternately up to the required range.

3.1. *Accuracy and stability*

The step-wise error in equation (15) is $O[(\Delta Z)^2]$. (If, at the last step, we apply the operator $\exp(\Delta ZA/2)$ instead of $\exp(\Delta ZA)$ then the scheme is equivalent to approximating $\exp(\Delta ZC)$ throughout by $\exp(\Delta ZA/2)\exp(\Delta ZB)\exp(\Delta ZA/2)$. This has a step-wise error of $O[(\Delta Z)^3]$, but globally is only marginally different). However, the overall accuracy depends on the degree of commutativity between A and B in the strong operator topology or, in other words, on the quantity $\|(AB-BA)m\|$. It is not difficult to show that this quantity is very small, and thus the method is highly accurate. Typically, for the chosen step sizes ΔZ, results were the same to within several decimal places as for step size $\Delta Z/2$. Since $(AB-BA)m$ is small these step sizes need not be prohibitively small. Accuracy is further confirmed by excellent agreement with analytical results and by the functional behaviour of σ_I^2 with Γ described in § 5.

The scheme is unconditionally stable and convergent, although some subtlety is needed in its application, particularly when there is very strong scattering. This solution, its accuracy, and the class of problems to which it applies will be dealt with in greater detail in another paper.

3.2. *Boundary conditions*

The limiting forms of $m(\xi,\eta)$ for large ξ and η are denoted by m_ξ and m_η. They correspond to the squares of the second moments and thus the boundary of any region will vary with respect to both ξ and η. It must therefore be treated analytically in order to approximate fully the Fourier transform of m by means of the FFT. We write $m_0 = m - m_\xi - m_\eta + m_{\xi\eta}$, where $m_{\xi\eta} = \lim_{\xi,\eta\to\infty} m(\xi,\eta)$. Then $m_0 \to 0$ at infinity. Also $\exp(\Delta ZA)m_0 = \exp(\Delta ZA)m$. Thus we can apply the FFT to m_0 instead of to m. In effect, the boundary is not changed by the diffraction operator. We subtract the boundary before applying $\exp(\Delta ZA)$ and add it afterwards, at each step.

3.3. *Autocorrelation function of the medium*

The method of operator splitting can be applied when the irregularities in the medium have any given autocorrelation function with an outer scale, even if it is range-dependent. The fourth-moment equation (3) was integrated numerically, using the above method, for the two autocorrelation functions $f(\xi)$ given below together with their corresponding spectra. The spectrum $F(\nu)$ is defined as follows

$$F(\nu) = \frac{1}{2\pi}\int_{-\infty}^{\infty} f(\xi)\exp(-i\nu\xi)\,d\xi. \tag{17}$$

(*a*) For a medium with a Gaussian spectrum

$$f(\xi) = \exp\{-\xi^2\},$$
$$F(\nu) = (1/2\sqrt{\pi})\exp\{-\nu^2/4\}, \tag{18}$$

(*b*) for a medium with a fourth-order power-law spectrum

$$f(\xi) = (1+|\xi|)\exp\{-|\xi|\},$$
$$F(\nu) = (2/\pi)[1+\nu^2]^{-2}. \tag{19}$$

The media represented by (18) and (19), which are physically very different, are chosen to illustrate the broad applicability of the numerical method. The medium with a Gaussian spectrum has irregularities with a single scale-size, whilst that with a

fourth-order power-law spectrum (19) has irregularities with a range of scale-sizes. Power-law spectra are characteristic of fractal-like structures, and in particular the spectrum (19) represents a sub-fractal medium (see Jakeman [14]).

4. Analytical solution of the fourth-moment equation

The numerical solutions of the fourth-moment equation (3) obtained by the method of operator splitting will be compared with existing analytical solutions. These consist of an expression giving the basic or fundamental form of the intensity fluctuation spectrum, and further expressions improving its accuracy. In the plane-wave geometry considered here the fundamental form of M, (13), is [1–4]

$$M_{(0)}(\nu, Z)=\frac{1}{2\pi}\int_{-\infty}^{\infty}\exp\left\{-2\Gamma\int_0^Z[1-g(\xi;\nu Z')]\,\mathrm{d}Z'\right\}\exp(\mathrm{i}\xi\nu)\,\mathrm{d}\xi. \tag{20}$$

The next higher-order term in the solution for M is [2, 4, 5]

$$\begin{aligned}M_{(1)}=\frac{4\Gamma}{2\pi}\int_0^Z\int\int_{-\infty}^{\infty}F(q)\sin^2\left(\frac{q\xi}{2}\right)\exp\left\{-2\Gamma\int_0^Z[1-g(\xi;\nu y)]\,\mathrm{d}y\right\}\\ \times\left[\exp\left(2\Gamma\int_0^S\{g[\xi+q(y-S);\nu y]-g(\xi;\nu y)\}\,\mathrm{d}y\right)-1\right]\\ \times\exp\{-\mathrm{i}\nu(\xi-qS)\}\,\mathrm{d}q\,\mathrm{d}\xi\,\mathrm{d}S.\end{aligned} \tag{21}$$

The analytical form of $M(\nu, Z)$ presented here is the approximation

$$M(\nu, Z)\approx M_{(0)}(\nu, Z)+M_{(1)}(\nu, Z). \tag{22}$$

At this point, we note that the fundamental form $M_{(0)}(\nu, Z)$ has now been derived by many authors using a variety of methods and in each case the result is identical. It is less clear that the higher-order corrections or additions to the fundamental are the same from author to author. The form (21) for $M_{(1)}$ given above has been derived by three completely different methods and the results have been shown to be identical. These results were obtained by summing the series solution of the fourth-moment equation [4], by the use of two-scale expansions [2] and by path-integral methods [5].

One of the aims of the present paper is to use the numerical solution for $M(\nu,Z)$ to investigate the adequacy with which the fundamental form $M_{(0)}$ represents $M(\nu, Z)$ and also to ascertain the accuracy with which the sum $M_{(0)}+M_{(1)}$ approximates $M(\nu, Z)$. It is a straightforward matter to evaluate $M_{(0)}$ (20). The procedure is still straightforward in the case of $M_{(1)}$ (21) but it is more computer-intensive. The integrals in the exponents can be evaluated analytically for the two autocorrelation functions employed here, and the integrand in S, which is evaluated last, turns out to be very smooth.

5. Results

5.1. *Scintillation index*

We now consider results of the numerical integration of the fourth-moment equation (3). The scintillation index σ_I^2 is presented first since it is a convenient quantity that allows us to illustrate the behaviour and stability of the numerical solution over a large range of values of Γ and Z. The spectrum (13) contains more

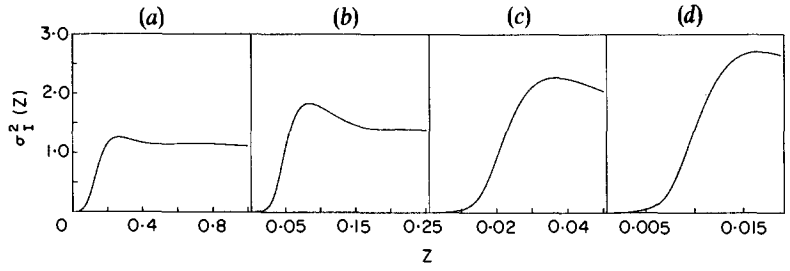

Figure 1. The scintillation index curve $\sigma_I^2(Z)$ obtained by solving (3) numerically with $f(\xi)$ given by (18) and the following values of Γ: (*a*) $\Gamma = 50$; (*b*) 1000; (*c*) 10 000; (*d*) 100 000.

information than its integral, the scintillation index. Spectra at selected distances Z for some values of Γ will be presented later.

Figure 1 shows $\sigma_I^2(Z)$ for the case when the autocorrelation function $f(\xi)$, (18), corresponds to inhomogeneities with a Gaussian spatial spectrum. The values of Γ presented range from 50 to 10^5, and the scaled distance Z is taken beyond the peak in σ_I^2. We note the smaller secondary peak in σ_I^2 for $\Gamma = 50$. This result has been obtained by other authors [7]. It is encountered only for low values of Γ and, apparently, only for single-scale inhomogeneities such as those described by the Gaussian autocorrelation function (18). The secondary peak vanishes for larger values of Γ, and σ_I^2 then decreases monotonically from its value at the main peak. For this reason the $\sigma_I^2(Z)$ curves are not presented for values of Z much beyond the peak, since, although the numerical integration is stable and well behaved, σ_I^2 falls off rather slowly in this region. In what follows we shall be particularly interested in the behaviour of the peak of $\sigma_I^2(Z)$ as a function of Γ.

Figure 2 shows $\sigma_I^2(Z)$ for the same range of values of Γ but for the case of the autocorrelation function $f(\xi)$ as given by (19), corresponding to the case of inhomogeneities with a fourth-order power-law spectrum. The general behaviour of the $\sigma_I^2(Z)$ curves is the same as in the previous case, the differences being clear from the figures.

The analytical form of $\sigma_I^2(Z)$ was evaluated from (10), (12) and (22) for $\Gamma = 50$, 1000 and the results are so close as to be indistinguishable from the numerical solutions in figures 1 and 2. The agreement between the numerical and analytical solutions is more easily seen by inspection of the corresponding spatial frequency spectra.

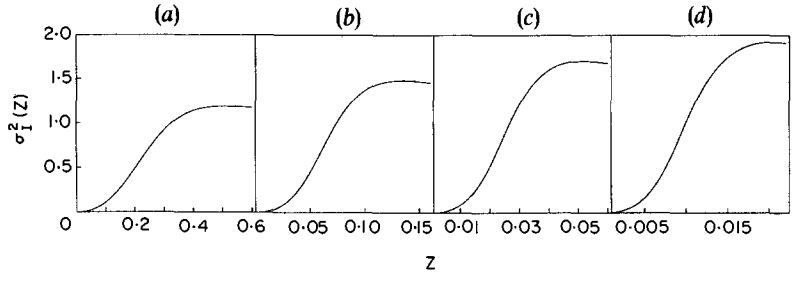

Figure 2. The scintillation index curve $\sigma_I^2(Z)$ obtained by solving (3) numerically with $f(\xi)$ given by (19) and the following values of Γ: (*a*) $\Gamma = 50$; (*b*) 1000; (*c*) 10 000; (*d*) 100 000.

5.2. *The spatial frequency spectra of intensity fluctuations*

The spatial frequency spectra $M(\nu, Z)$ for a medium with the Gaussian autocorrelation function (18) are given in figure 3 for $\Gamma = 50$ and in figure 4 for $\Gamma = 1000$. In both cases the values of Z chosen are approximately 0·5, 1·0 and 1·5 times the depth at which σ_I^2 has its maximum value. The spectra obtained by solving the fourth moment equation numerically are shown by the full lines, while the theoretical spectra obtained by evaluating expressions (20)–(22) are given by the broken lines. The agreement is seen to be very good. The discrepancy that appears for larger values of Z is similar for both values of Γ presented here. This discrepancy increases for larger values of Γ and may be an indication that higher-order terms need to be taken into account in the theoretical spectra.

The corresponding numerical and theoretical spectra for a medium having a fourth-order power-law spectrum, (19), of inhomogeneities are given in Figures 5 for $\Gamma = 50$ and in Figures 6 for $\Gamma = 1000$. As before, the distances Z selected are approximately 0·5, 1·0 and 1·5 times the distance to the maximum of σ_I^2. Once again the agreement between the analytical and numerical results is good.

5.3. *Accuracy of the theoretical spectra*

The availability of an accurate numerical solution of the fourth-moment equation over a large range of values of Γ and Z allows us to answer some important questions as to the accuracy and adequacy of the existing theoretical solutions. The first question concerns the accuracy of the theoretical spectrum (22), the sum of the two approximations (20) and (21). It is clear from the results of the previous section that the sum (22) approximates the numerical solution very accurately for values of Γ up to 1000. The approximation is less good for larger values of Γ.

5.4. *Usefulness of the fundamental form*

The second question that our accurate numerical solution can help to answer is whether the fundamental approximation (20) can validly be employed to study the intensity fluctuation spectrum and, if so, under what conditions. It is important to know this, since the higher-order correction has a complicated analytical form that does not readily yield physical insight. It is worthwhile noting that the fundamental form (20) is a good approximation even for very large values of Γ, when Z is either less than one-half the distance to the scintillation index peak or else is extremely large, since in both these cases it can be shown that the higher-order corrections tend to zero.

The discrepancy between the fundamental form of the spectrum (20) and the accurate numerical solution is greatest for values of Z close to the peak in $\sigma_I^2(Z)$. The fundamental form of the spectrum preserves the shape and overall behaviour of the numerical spectrum for all values of Γ, Z and so is extremely valuable for gaining insight into these. However, the integrated value of the fundamental spectrum, that is the scintillation index $\sigma_{I(1)}^2$, falls short of that obtained from the numerical spectrum, $\sigma_{I(2)}^2$. This discrepancy evaluated at the peak of σ_I^2 and expressed as a fraction of the peak value,

$$\Delta(\Gamma) = 1 - (\sigma_{I(1)}^2/\sigma_{I(2)}^2), \tag{23}$$

is a measure of the adequacy with which the fundamental form (20) approximates the accurate numerical spectrum.

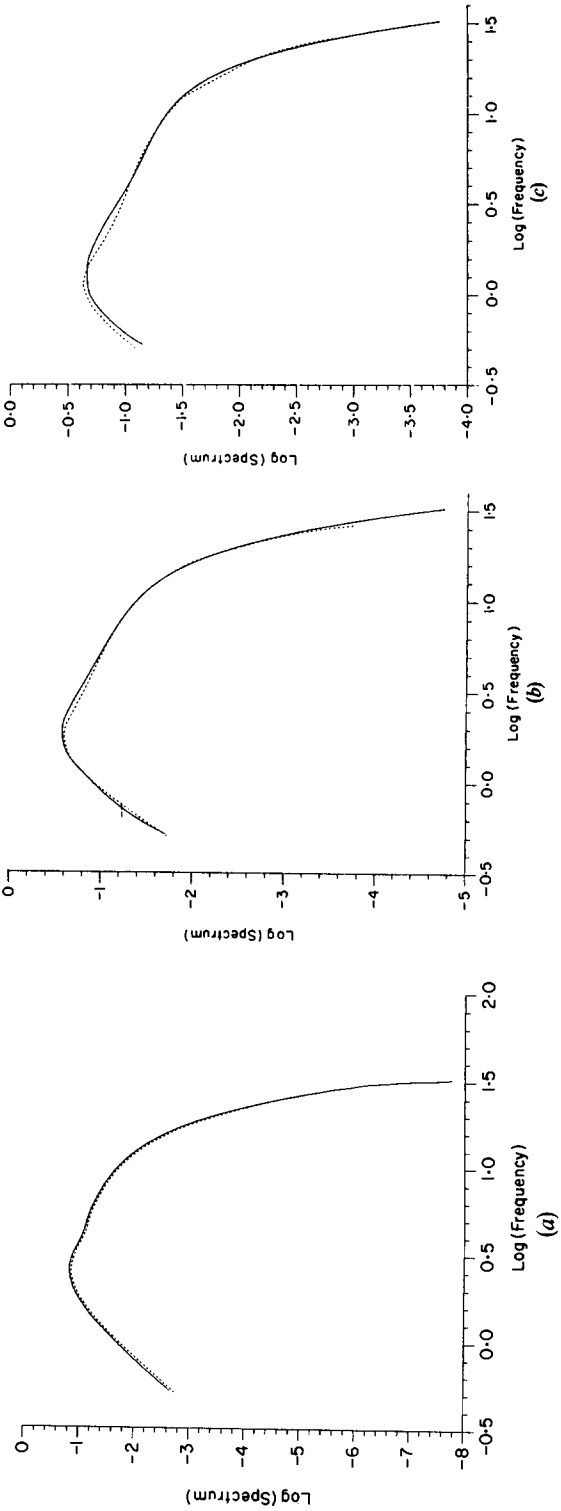

Figure 3. The spatial frequency spectra $M(\nu, Z)$ for a medium with $f(\xi)$ given by (18) and $\Gamma = 50$. The full and broken curves correspond to the numerical and theoretical solutions respectively. The distances Z are (*a*) $Z \approx 0{\cdot}5Z_{f_0}$, (*b*) Z_{f_0} and (*c*) $1{\cdot}5Z_{f_0}$, where Z_{f_0} is the position of the scintillation index peak.

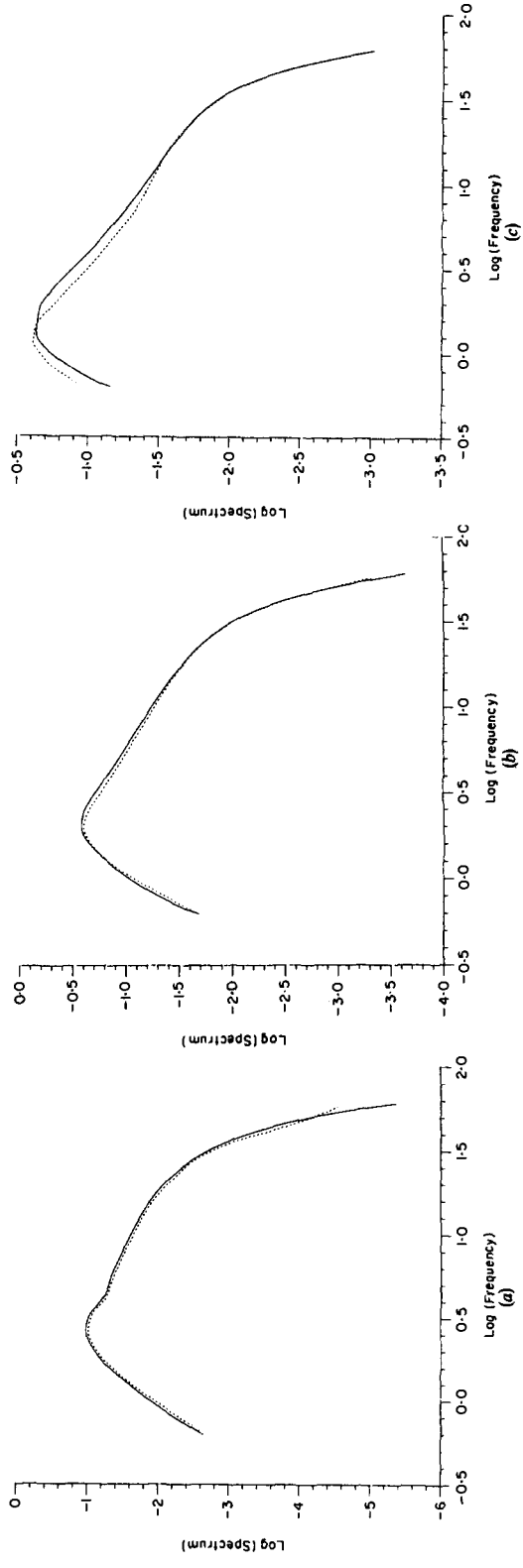

Figure 4. The same as in figure 3 but with $\Gamma = 1000$. The distances Z are (*a*) $Z \approx 0{\cdot}5Z_{fo}$, (*b*) Z_{fo} and (*c*) $1{\cdot}5Z_{fo}$.

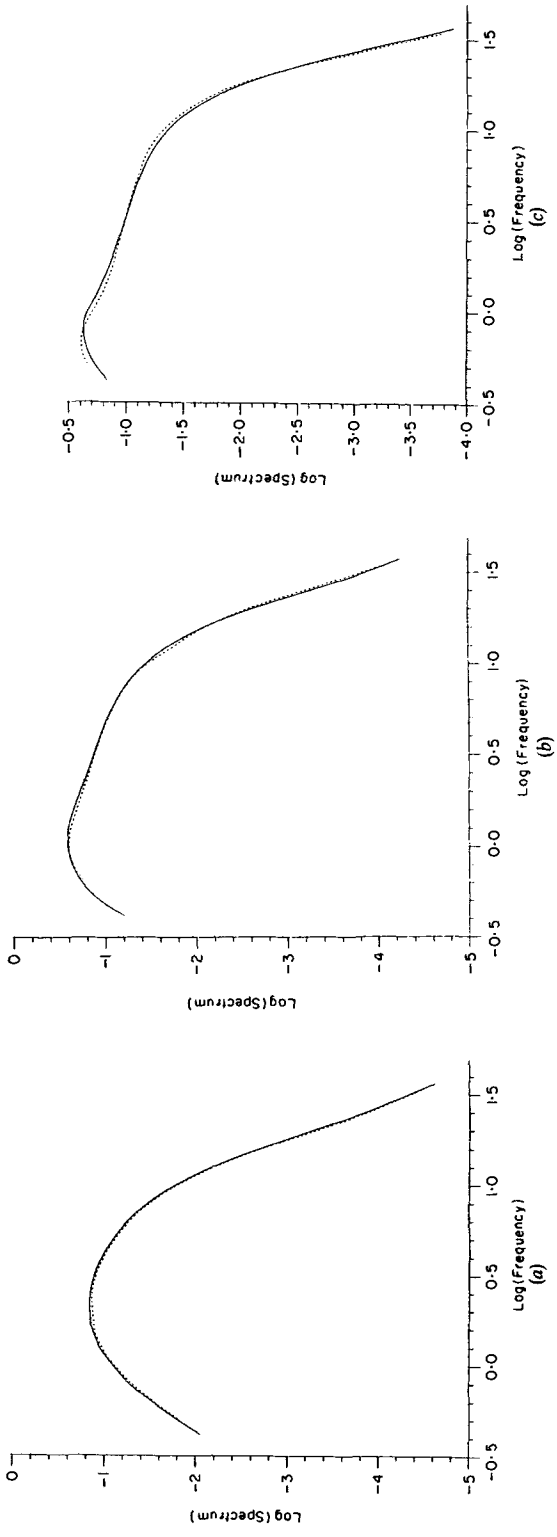

Figure 5. The spatial frequency spectrum $M(\nu, Z)$ for a medium with $f(\xi)$ given by (19) and $\Gamma = 50$. The full and broken curves correspond to the numerical and theoretical solutions respectively. The distances Z are (*a*) $Z \approx 0{\cdot}5 Z_{f_0}$, (*b*) Z_{f_0} and (*c*) $1{\cdot}5 Z_{f_0}$.

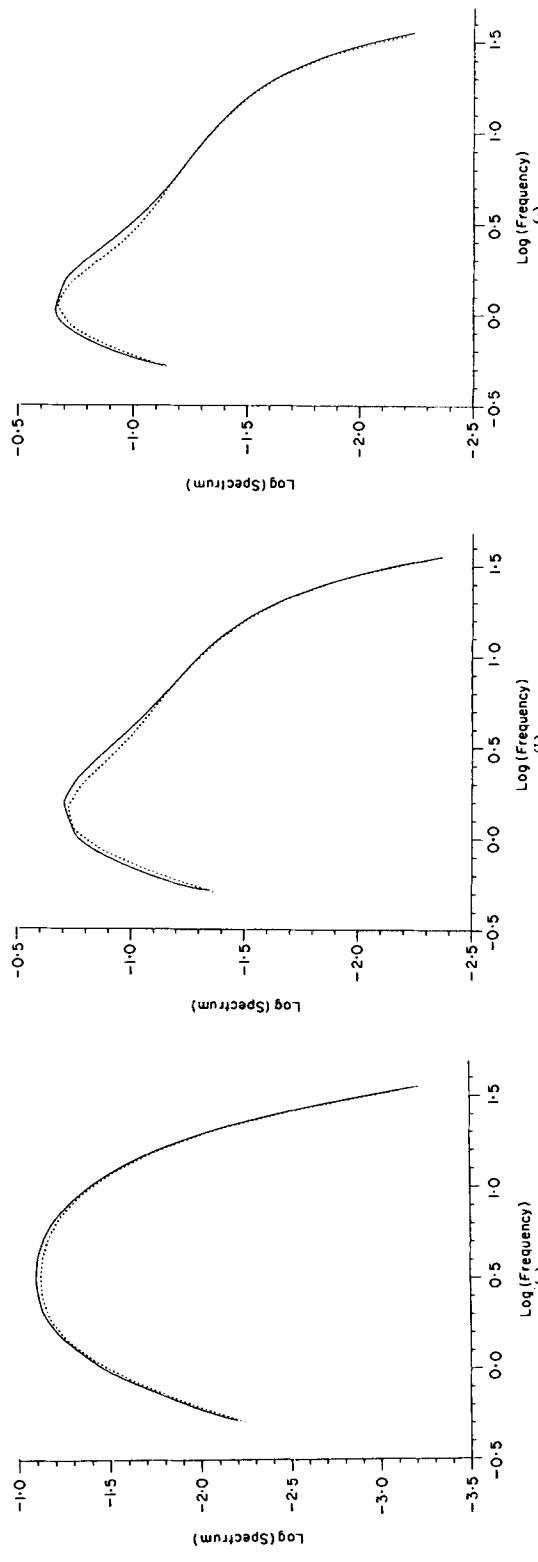

Figure 6. The same as in figure 5 but with $\Gamma = 1000$. The distances Z are (*a*) $Z \approx 0{\cdot}5 Z_{f_0}$, (*b*) Z_{f_0} and (c) $1{\cdot}5 Z_{f_0}$.

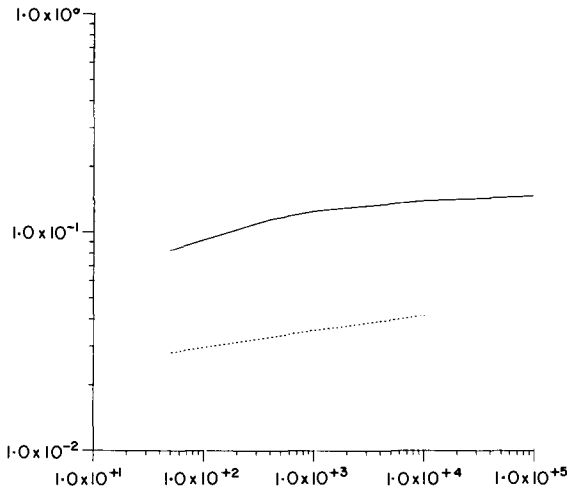

Figure 7. The discrepancy in a medium with Gaussian autocorrelation function between the scintillation-index peak computed numerically and the theoretical value resulting from (*a*) the fundamental alone $\Delta(\Gamma)$ (full line) and (*b*) the fundamental and correction $\Delta'(\Gamma)$ (broken line).

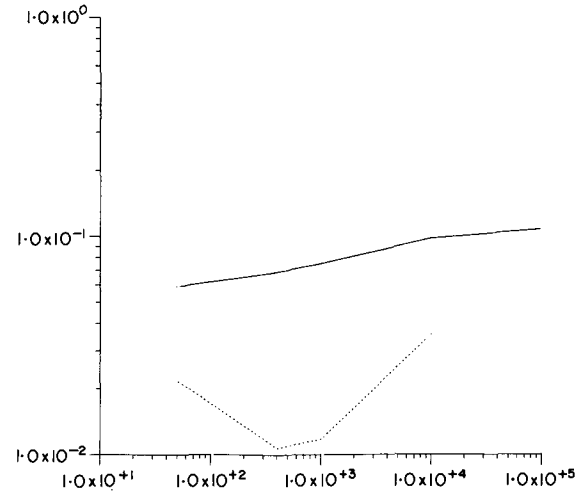

Figure 8. The same as in figure 7 for a medium with $f(\xi)$ given by (19).

Figure 7 shows $\Delta(\Gamma)$ for a range of values of Γ for a medium with Gaussian autocorrelation function. We see that the fractional discrepancy remains roughly constant. It will be shown below that $\Delta(\Gamma)$ tends to a constant for very large Γ. This leads us to the conclusion that the fundamental form of the spectrum can be used to investigate all the main characteristics of the accurate numerical solution with a maximum integrated error of about 14%.

The same procedure can be repeated with the corrected form of the theoretical spectrum (22). Let the discrepancy between the theoretical scintillation index at the

peak and the numerical solution, expressed as a fraction of the numerical solution, be $\Delta'(\Gamma)$. This is then a measure of the accuracy of (22). $\Delta'(\Gamma)$ is also shown in figure 7. The discrepancy is much less when the first-order correction is included, although it does not appear to level off as Γ increases. Figure 8 shows the same quantities for a medium with autocorrelation function (19). Here the behaviour of $\Delta'(\Gamma)$ is less systematic. This is due partly to the high accuracy of the expression (22) and partly to its computational difficulty.

5.5. *Behaviour of the scintillation-index peak*

Let the value of Z at which the scintillation-index peak occurs be Z_{f_0}. The height of this peak is then $\sigma_I^2(Z_{f_0})$. We conclude this paper by showing that there exist simple laws governing the position and height of the peak. The following approximate analytical expression for the scintillation index can be obtained [1] by integrating the fundamental form of the spectrum in the case of the medium with the autocorrelation function (18).

$$\sigma_{I(1)}^2 = \tfrac{2}{3}\Gamma Z^3\left\{6\,\mathrm{erf}\left[\frac{1}{(4\Gamma Z^3)^{1/2}}\right] - \frac{2}{(\pi\Gamma Z^3)^{1/2}}\exp\left[\left(-\frac{1}{4\Gamma Z^3}\right)\right]\left(3+\frac{1}{2\Gamma Z^3}\right)\right\}$$
$$+\frac{1}{(8\pi\Gamma Z^3)^{1/2}}\exp\left(-\frac{1}{8\Gamma Z^3}\right)\ln(\Gamma Z)+\left\{1-\mathrm{erf}\left[\frac{1}{(8\Gamma Z^3)^{1/2}}\right]\right\}. \quad (24)$$

It is clear that, for large values of Γ, the peak in σ_I^2 is chiefly due to the term involving $\ln(\Gamma Z)$. Differentiation of this term with respect to Z shows that the peak occurs approximately when $4\Gamma Z^3$ is equal to unity. We can thus expect the peak in the scintillation index to lie in the region of

$$Z_{f_0} \approx 0{\cdot}65\Gamma^{-1/3}, \quad (25)$$

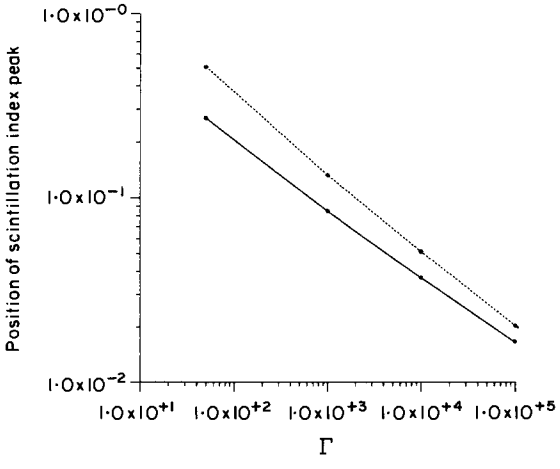

Figure 9. Position of the scintillation-index peak Z_{f_0} for a random medium with autocorrelation function $f(\zeta)$, as given by (18) (full line) and (19) (broken line), as the value of Γ increases.

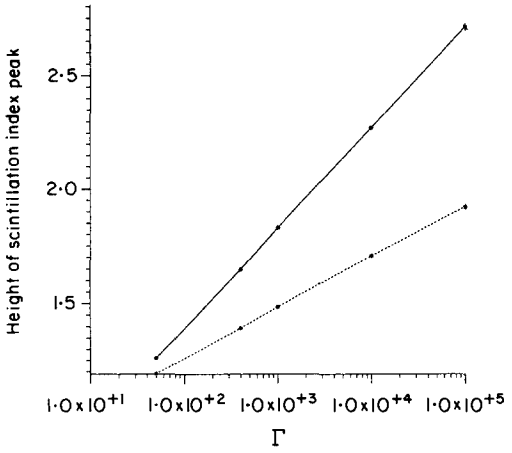

Figure 10. Height of the scintillation-index peak $\sigma_I^2(Z_{f_0})$ for a random medium with autocorrelation function $f(\xi)$ as given by (18) (full line) and (19) (broken line), as the value of Γ increases.

while substitution of (25) into (24) indicates that the height of the peak behaves approximately as

$$\sigma_I^2(Z_{f_0}) \approx 0{\cdot}437 + 0{\cdot}161 \ln \Gamma. \tag{26}$$

The validity of these simple laws, derived on the basis of the fundamental form, can now be tested by using the accurate numerical solution. The curve for Z_{f_0} obtained from the numerical results is given by the full line in figure 9. The curve is well represented, especially for large values of Γ, by

$$Z_{f_0} \approx 0{\cdot}84\Gamma^{-0{\cdot}34} \tag{27}$$

while the height of the peak turns out to be, (figure 10 (full line)),

$$\sigma_I^2(Z_{f_0}) = 0{\cdot}56 + 0{\cdot}185 \ln \Gamma. \tag{28}$$

The similarity between the numerically derived laws (27) and (28) and the analytical forms (25) and (26) is further evidence of the way in which the fundamental form of the spectrum tracks the numerical result, and of the usefulness of this simple analytical form. The limit, as Γ tends to infinity, corresponds to the short-wavelength limit. Several authors (see for example Berry [13], and Jakeman [14]) have considered such laws for the short-wave limit in the geometrical optics regime. (The form (25), which corresponds to a constant physical distance z_{f_0}, can be derived in this way). The present method, not restricted to the geometrical optics regime, is applicable to values of Γ far removed from the short wavelength limit. Thus the region of applicability of these laws is considerably extended. The accuracy and stability of the numerical laws for the numerical solution over such large ranges of Γ is remarkable. We are prompted to draw the conclusion that such laws hold more generally, over a wide class of media. An estimate of the fractional discrepancy between the accurate numerical solution and that derived from the fundamental form can be obtained by setting (26) and (28) in (23). It turns out that $\Delta(\Gamma)$ approaches a constant value of about 0·133 for large Γ.

A similar procedure can be followed for the medium with the autocorrelation function (19). The fundamental form of the intensity fluctuation spectrum can once again be integrated to give an analytical expression for the scintillation index. This yields laws similar to (25), (26) for the behaviour of the position and height of the peak. In this case the numerical laws obtained from the numerical solution are once again close to the analytical results and are

$$Z_{f_0} = 2{\cdot}5\Gamma^{-0{\cdot}425}, \tag{29}$$

$$\sigma_I^2(Z_{f_0}) = 0{\cdot}83 + 0{\cdot}095 \ln \Gamma. \tag{30}$$

The dependences (29), (30) obtained from the numerical solution of (3) are shown by the broken lines in figures 9 and 10, respectively.

Acknowledgment

This work was supported by the Ministry of Defence (Procurement Executive).

References

[1] Uscinski, B. J., 1982, *Proc. R. Soc., Lond.*, **380,** 137.
[2] Macaskill, C., 1983, *Proc. R. Soc., Lond.*, **386,** 461.
[3] Frankenthal, S., Whitman, A. M., and Beran, M. J., 1984, *J. opt. Soc. Am.* A, **1,** 585.
[4] Uscinski, B. J., 1985, *J. opt. Soc. Am.* A, **2,** 2077.
[5] Uscinski, B. J., Macaskill, C., and Spivack, M., 1986, *J. Sound Vibration*, **106,** 509.
[6] Dagkesamanskaya, I. M., and Shishov, V. I., 1970, *Radiophys. quant. Electron.*, **13,** 9.
[7] Tur, M., 1982, *J. opt. Soc. Am.*, **72,** 1683.
[8] Gozani, J., 1985, *J. opt. Soc. Am.* A, **2,** 2144.
[9] Brown, Jr., W. P., 1972, *J. opt. Soc. Am.*, **62,** 966.
[10] Shishov, V. I., 1971, *Zh. éksp. teor. Fiz.*, **61,** 1399.
[11] Macaskill, C., and Ewart, T. E., 1984, *IMA J. appl. Math.*, **33,** 1.
[12] Tappert, F. D., and Hardin, R. H., 1974, *Proceedings of the Eighth International Congress on Acoustics*, Vol. II (London: Goldcrest).
[13] Berry, M. V., 1977, *J. Phys.* A: *Math. Gen.*, **10,** 2061.
[14] Jakeman, E., 1987, *Conference on Scattering and Propagation in Random Media*, edited by K. C. Yeh (Neuilly-sur-Seine: AGARD).